Gu, Z., Yan, S., Cheong, S., Cao, Z., Zuo, H., Thomas, A. C., Rolfe, B. E., & Xu, Z. P. (2018). Layered double hydroxide nanoparticles: Impact on vascular cells, blood cells and the complement system. *Journal of Colloid and Interface Science*, *512*, 404-410. https://doi.org/10.1016/j.jcis.2017.10.069

Layered double hydroxide nanoparticles: Impact on vascular cells, blood cells and the complement system

Zi Gu*[,a], Shiyu Yan[b], Soshan Cheong[c], Zhengbang Cao[a], Huali Zuo[b], Anita C. Thomas[d], Barbara E. Rolfe*[,b] and Zhi Ping Xu*[,b]

[a]*School of Chemical Engineering, Australian Centre for NanoMedicine (ACN), The University of New South Wales, Sydney, NSW 2052, Australia*

[b]*Australian Institute for Bioengineering and Nanotechnology, The University of Queensland, Brisbane, QLD 4072, Australia*

[c]*Electron Microscope Unit, The University of New South Wales, Sydney, NSW 2052, Australia*

[d]*Bristol Heart Institute & Bristol CardioVascular, University of Bristol, Bristol, BS2 8HW, United Kingdom*

* Joint senior authors, to whom correspondence should be addressed. E-mail: Dr Zi Gu (zi.gu1@unsw.edu.au), Dr Barbara Rolfe (b.rolfe@uq.edu.au), Prof Zhi Ping Xu (gordonxu@uq.edu.au),

Keywords: layered double hydroxide, biosafety, vascular cells, cell proliferation and viability, cell migration, haemolysis, complement activation

Abstract

The mounting interest in layered double hydroxide (LDH) nanoparticles as drug carriers and bio-imaging contrast agents makes biosafety evaluation of LDH essential. Considering the important role of blood circulation in bio-distribution of nanoparticles, the present work evaluated the impact of MgAl-LDHs on key components of the circulatory system, including vascular cells (vascular smooth muscle cells (SMCs) and endothelial cells (HUVECs)), red blood cells (RBCs), and complement activation. The results showed that LDH had no effects on SMCs and HUVECs at concentrations up to 500 and 10 μg/mL respectively, in terms of cell proliferation and viability. LDH (10 μg/mL) did not change either the migration distance or the number of migrating SMCs in culture. Moreover, LDH (400 μg/mL) had a negligible effect on RBCs' lysis, and there was no significant increase in levels of complement activation product, C5a, in the presence of LDH (20 or 200 μg/mL). The low toxicity for vascular cells and blood cells combined with low immunogenicity sheds a light on the biosafety of LDH nanoparticles, and encourages further studies into their biomedical applications.

1. Introduction

Biomedical applications of nanoparticles as drug delivery agents and bio-imaging contrast agents have attracted mounting interest [1], which results in an urgent need for biosafety evaluation to understand the effect of nanoparticles on biological systems. Studies to address the potential toxicity of nanoparticles are limited in comparison with the increased number of nanoparticle types and applications, and there is a considerable amount of work to be done in order to fully assess the toxicity of these nanomaterials. Intravenous injection and oral administration are two major exposure pathways of therapeutic/diagnostic nanoparticles. For intravenously injected nanoparticles, vascular components, including blood cells, vascular cells and serum proteins, are the first contact. The blood also plays a vital role for orally administered nanoparticles, as the nanoparticles cannot reach their target tissues and cells without first passing through blood. However, the influence of nanoparticles on vascular components is not well understood.

Layered double hydroxides (LDHs) are a family of hydrotalcite-like materials [2]. They consist of metal hydroxide layers (e.g. $Mg_2Al(OH)_6^+$) and interlayer spacing containing anions (e.g. Cl^-, NO_3^-, CO_3^{2-}) and H_2O [2]. The typical morphology of LDHs is a hexagonal plate-like sheet with the lateral diameter of approximately 50-200 nm [2]. The unique properties of layered double hydroxide (LDH) nanoparticles, including facile isomorphic substitution, internalization of guest molecules for sustained release, pH sensitivity, and easy hybridization with other nanoparticles to form multi-functional nanocomposites [3-6], pointing to their therapeutic and diagnostic potential. A variety of therapeutic agents, including drug molecules, siRNA and antibodies have been coupled with LDHs, and shows excellent results in sustained release, target delivery, cellular uptake and immune responses [7-15]. We previously reported that the intravenous injection of LDH nanohybrids intercalated with an anti-coagulant drug

prevented the luminal loss and the thrombus development in a rat model of balloon angioplasty [16]. LDH is also a very promising bio-imaging contrast enhancer. Very recently we developed manganese-doped LDHs and radiometal-doped LDHs which showed clear magnetic resonance imaging and positron emission tomography imaging respectively after intravenous injection in animal models [17, 18]. Combining the therapeutic and diagnostic agents on a single LDH nanoplatform promises to facilitate personalized medicine.

Despite of a number of studies on the LDHs' therapeutic and diagnostic functions, investigations on the impact of LDH nanoparticles on vascular components are very limited. Herein we reported our studies on the potential toxicity of MgAl-Cl-LDH nanoparticles towards rat vascular smooth muscle cells (SMCs), human umbilical vein endothelial cells (HUVECs) and red blood cells (RBCs). We also investigated the potential for LDH nanoparticles to activate the complement system, a key component of innate immunity and known to mediate the earliest responses to foreign materials injected into the blood stream [19]. We propose that these *in vitro* and *ex vivo* data could be used as an initial screen for biosafety of nanoparticles.

2. Materials and Methods

2.1 Synthesis and characterization of LDH nanoparticles

MgAl-Cl-LDH (LDH) nanoparticles were synthesized using a co-precipitation method described previously [9]. Briefly, 0.17 M NaOH (Labscan, 99.0%) solution (40 mL) was vigorously stirred with a mixed solution (10 mL) containing 0.3 M $MgCl_2 \cdot 6H_2O$ (Fluka, 98.0%) and 0.1 M $AlCl_3 \cdot 6H_2O$ (Fluka, 99.0%). The precipitate was separated and washed twice by

centrifugation before hydrothermal treatment at 100 °C for 16 h. For incubation with whole blood, LDH synthesis was carried out under sterile conditions (in a laminar flow hood) using uncontaminated chemicals and nuclease-free H_2O (Ambion®).

Transmission electron microscopy (TEM) images were obtained on a Phillips CM200 operated at 200 kV. Scanning transmission electron microscopy coupled with energy dispersive X-ray spectroscopy (STEM-EDS) analysis was carried out on a JEOL JEM-F200 (at 200 kV) equipped with a windowless JEOL silicon drift detector (SDD). EDS data was analysed using the NSS Noran System 7 Software (Thermo Scientific). Particle size distribution and zeta potential were measured by dynamic light scattering using a Nanosizer Nano ZS instrument (Malvern Instruments). The size distribution was derived from the experimental autocorrelation function of the scattered intensity through a general purpose (normal resolution) analysis model. Powder X-ray diffraction (XRD) patterns were recorded on a Rigaku Miniflex X-ray Diffractometer using Co Kα source (λ = 0.178897 nm) at a scanning rate of 0.02°/s (2θ) from $2\theta = 2^o$ to $2\theta = 80^o$.

2.2 Cell culture

Isolation and culture of primary rat vascular SMCs were described previously [8]. For all experiments cells between the 2nd and 6th passage were seeded in 90 mm petri dishes, 6-well or 24-well tissue culture plates at a density of 10^5 cells/cm^2 in growth medium (M199 plus 10% fetal calf serum containing penicillin and streptomycin; Invitrogen), and incubated at 37 °C in a humidified atmosphere of 5% CO_2 in air.

Primary human umbilical vein endothelial cells (HUVECs) were provided by Lonza and used at passages up to 6. Cells were seeded at 10^5 cells/cm^2 in growth medium (RPMI 1640 plus 10% fetal calf serum, endothelial cell growth supplement (100 μg/mL), heparin (200 μg/mL) as well as penicillin and streptomycin; Invitrogen) at 37 ˚C in a humidified atmosphere of 5% CO_2 in air.

2.3 Cell proliferation and viability

The proliferation and viability of cultured SMCs or HUVECs were assessed using the Trypan Blue dye exclusion test. When cultured cells reached 70~80% confluence, growth medium was replaced with fresh medium containing LDH nanoparticles at concentrations from 0 to 500 μg/mL (concentrations previously tested for *in vitro* studies, and much higher than we have found to be effective *in vivo*) [8, 16]. Twenty-four or forty-eight hours after treatment, cells were harvested and examined for their ability to exclude Trypan Blue (Sigma-Aldrich). Viable (dye excluding) and non-viable (dye including) cells were counted using a hemocytometer. At each time point, the proportion of viable cells was compared with controls, and the ratio of viable cells to total cell number at each time point indicated the cell viability.

2.4 Cell migration

The influence of LDH nanoparticles on SMC migration was investigated using a scrape injury method [20]. Confluent SMC cultures were pre-treated with hydroxyurea (5 mmol/L; Sigma) to prevent cell proliferation, and then the cells in the centre of the well scraped off. After washing, fresh growth medium containing hydroxyurea and LDH suspension (10 μg/mL) was added to the cell culture. Control cultures were grown in growth medium containing

hydroxyurea alone. The wounds were photographed under an Olympus IX81 microscope at the time of scraping and again after 4 days. At this time, the cytoplasm and nuclei of attached cells were stained with CellTracker Green (Molecular Probes) and Hoechst 33342 (Molecular Probes) respectively, and fluorescence images superimposed on the transmitted light images taken at the same position. The number of migrated cells was counted, and the migration distance measured as the vertical distance from the cell to the scratch line closer to the cell population.

2.5 Haemolysis assay

Ethylenediamine tetraacetic acid (EDTA; Sigma)-stabilized blood samples were freshly obtained from C57BL/6 male mice. RBCs were isolated from blood by centrifugation at 10016 g for 10 min, followed by five times washing with phosphate buffered saline (PBS; Invitrogen). The washed RBCs were suspended in PBS, and added to the nanoparticle suspension in a volume ratio of 1:4 to give a final nanoparticle concentration of 25-400 μg/mL. RBCs incubated with distilled water or PBS were used as the positive and negative controls respectively. After static incubation at 37 $^{\circ}$C for 3 h, the samples were centrifuged at 10016 g for 3 min, the supernatant collected and the absorbance at 570 nm measured on a microplate reader (BioTek), with absorbance at 655 nm as a reference. The percent haemolysis of RBCs was calculated using the formula: ((sample absorbance - negative control absorbance) / (positive control absorbance - negative control absorbance)) × 100 [21, 22].

2.6 Complement activation assay

The capacity for LDH nanoparticles to induce complement activation was determined in an *ex vivo* assay using anti-coagulated mouse plasma (a modification of the method described by Mollnes *et al.*) [23]. Mouse blood was harvested from healthy mice via cardiac puncture into tubes containing thrombin inhibitor lepirudin (50 μg/mL blood; Hoechst AG), an anti-coagulant that does not interfere with complement activation [23]. The plasma was collected and dispensed into sterile 0.5 mL tubes (45 μL/test). To each tube was added 5 μL of PBS alone (negative control), or PBS containing zymosan (20 μg/mL plasma; positive control; Sigma) or LDH nanoparticles prepared under endotoxin-free conditions (20 or 200 μg/mL plasma), and samples gently mixed at 37 °C for 0.5 or 2 h. Reactions were terminated by adding protease inhibitor FUT-175 (0.1 mg/mL plasma; BD Pharmingen) and EDTA (3 mg/mL plasma). For the zero time-point (negative control), FUT-175 and EDTA were added to plasma before addition of nanoparticles and incubated for 2 h. Each sample was then centrifuged to remove nanoparticles, and the supernatant stored at -80 °C until analysis.

The complement activation product C5a was measured by Enzyme-Linked Immunosorbant Assay (ELISA) [24]. Purified rat anti-mouse C5a capture antibody (Clone I52-1486; BD Pharmingen) diluted in coating buffer (100 μM $NaHCO_3$ 34 μM Na_2CO_3, pH 9.5) was coated onto high affinity binding 96-well plates (Greiner Bio-one) and incubated overnight at 4°C. After blocking non-specific binding with PBS/10% fetal calf serum, a standard curve was prepared by two-fold dilution of purified recombinant mouse C5a (BD Pharmingen). Serum samples (diluted 1:50 or 1:25 in PBS containing 10% fetal calf serum) were added to duplicate wells and incubated for 2 h at room temperature. The wells were then incubated with detection antibody (biotinylated rat anti-mouse C5a; Clone I52-278; BD Pharmingen) for 1 h at room temperature, followed by a 0.5 h incubation with streptavidin-horseradish peroxidise conjugate (BD Pharmingen), and then 3,3',5,5'-tetramethylbenzidine substrate (Sigma-Aldrich) for 0.5

h. The reaction was stopped by addition of 1 M H_2SO_4, and absorbance at 450 nm wavelength measured on a microplate reader (BioTek).

2.7 Statistical analysis

Data are expressed as mean ± SEM. Arc Sine square root transformation was applied where appropriate. Differences between the treatments were analyzed by one-way or two-way ANOVA followed by Sidark's multiple comparisons test using GraphPad Prism software. A p value ≤ 0.05 was considered statistically significant.

3. Results and discussion

3.1 Physicochemical features of LDHs

The structural characteristics of MgAl-Cl-LDH nanoparticles prepared by the co-precipitation method were shown in Fig. 1. The typical hexagonal platelet shape of the LDH particles with the lateral diameter from 50-150 nm was observed from the TEM image (Fig. 1A). Scanning transmission electron microscopy-energy dispersive X-ray spectroscopy (STEM-EDS) elemental mappings of Mg, Al and O demonstrated the uniform distribution of metal and oxygen elements in the LDH platelet matrix (Fig. 1 B-E). Hydrodynamic size analysis showed a single, sharp peak with an average particle diameter of 116 ± 2 nm and a polydispersity index of 0.14 ± 0.01 (Fig. 1F), demonstrating that LDH nanoparticles were homogeneously dispersed in water. The correlation curve of size distribution was shown in Fig. S1. LDH nanoparticles had an average zeta potential of 39 ± 1 mV. The XRD pattern (Fig. 1G) is typical of well-crystallised lamellar materials, and characterized with the sharp (003) and (006) basal reflections and two separated (110) and (113) peaks. The interlayer spacing ((003) spacing) of

the LDH particle was calculated to be 0.77 nm, corresponding to the previously reported Cl^- intercalated LDH [25].

3.2 Influence of LDH nanoparticles on vascular cell proliferation, viability and migration

Proliferation and migration are two important indexes of cell growth. As shown in Fig. 2A, the number of viable SMCs in the control group (0 μg/mL LDH) increased by 235 ± 1% and 364 ± 24% after 24 and 48 h incubation respectively. The proliferation rates of SMC cultures treated with 10-500 μg/mL LDH did not differ significantly from that of control cultures at every time point. However, the average value of the proliferation rate for cells treated with 500 μg/mL LDH group was lower than that in cultures treated with either 10 or 100 μg/mL LDH. In contrast, the number of viable HUVECs in control cultures increased by 310 ± 70% during the 2 day incubation (Fig. 2B). Cultures treated at the LDH concentration of 10 μg/mL had a similar increase in the number of viable cells over the same time period and were not significantly different from control cultures. At higher LDH concentrations (50 and 100 μg/mL) the HUVEC number of did not obviously increase over the 2 day treatment period, but was significantly lower than that in the control cultures ($p<0.01$).

SMC viability in the control group was greater than 90% throughout the 2-day incubation period (Fig. 2C), and was not affected by LDH at concentrations up to 500 μg/mL. Cell viability for HUVEC cultures treated with 0 or 10 μg/mL LDH remained around 90% throughout the 2-day treatment period (Fig. 2D). However, higher LDH concentrations resulted in significant reductions in cell viability, to 61 ± 1% ($p<0.0001$) and 36 ± 3% ($p<0.0001$) respectively for LDH concentrations of 50 and 100 μg/mL after 48 h. Compared with SMCs, HUVECs are more sensitive to LDH treatment. Since endothelial cells lining blood vessel walls are likely to be among the first cells to encounter nanoparticles following intravenous injection, the LDH

dose should be limited to ensure that the concentration in blood is below 50 μg (nanoparticles)/mL, in order to avoid damage to the blood vessel wall. However, local delivery techniques (such as perivascular delivery) may still allow the use of higher LDH doses as a therapy.

In the migration study (Fig. 3A), following scrape injury, SMCs moved across the scratch line and spread into the scraped area of the well. Cell morphology changed from spindle-like to a fan-shape with large lamellipodia, indicative of cell motility. By day 4, treatment with LDH (10 μg/mL) resulted in a slight reduction in both the number of cells migrating into the scraped area (83 ± 8%) and the average migration distance (92 ± 10%), compared with control treatment (Fig. 3B).

3.3 Haemolytic activity of LDH nanoparticles

Erythrocytes play a vital role by delivering oxygen to organs and tissues via the circulatory system. Haemolysis can lead to life-threatening conditions, such as hemolytic anemia, jaundice and renal failure. Spectrophotometric analysis of supernatants following exposure of whole blood to LDHs for 3 h showed a slight increase in haemolysis (from 0.2 ± 0.5% to 4.3 ± 0.1%) as the LDH concentration increased from 25 to 400 μg/mL, but this was not significant ($p = 0.35$) (Fig. 4B). The results suggest that LDH at concentrations up to 400 μg/mL does not cause significant haemolysis.

3.4 Complement activation by LDH nanoparticles

Complement activation is responsible for inflammation, tissue injury and hypersensitivity [26, 27]. Upon entering the bloodstream, all foreign materials are immediately recognized by the complement system [19], leading to the generation of potent activation products including

opsonin C3b and anaphylatoxin C5a. Surface coating ('opsonization') of nanoparticles with C3b leads to recognition by myeloid cells (neutrophils, monocytes, macrophages) [28], subsequent removal by phagocytosis, pinocytosis or endocytosis [29], and clearance to lymphoid organs (liver, spleen, lymph nodes) [19]. The rapid uptake of nanoparticles by phagocytic cells reduces their circulation time and is thought to be a major cause of reduced therapeutic efficacy of injected nanoparticles [30]. C5a is a potent chemoattractant for neutrophils and monocyte/macrophages, and also triggers the release of secondary pro-inflammatory mediators (the 'cytokine storm') [31]. This can induce adverse hypersensitivity responses, such as those reported to occur in 45% of patients treated with liposomal doxorubicin [32].

Analysis of anti-coagulated mouse plasma showed that the concentration of the activation product C5a at the zero time point (0 h, before addition of LDH nanoparticles) was approximately 8 ng/mL. The level of C5a increased in all treatment groups during the 2 h incubation period. Half an hour and 2 h after addition of zymosan (20 μg/mL; positive control), plasma C5a levels were 212 ± 74 and 338 ± 45 ng/mL respectively, indicating significantly enhanced activation of complement in relation to untreated and PBS-treated control groups. In contrast to zymosan, LDH was much less effective in activating complement, indicated by C5a levels of 81 ± 36 ng/mL (20 μg/mL LDH) and 80 ± 13 ng/mL (200 μg/mL LDH) after 2 h incubation, not significantly different from the untreated (42 ± 11 ng/mL) and PBS-treated (21 ± 1 ng/mL) control groups after 2 h incubation. These results show no significant complement activation following exposure to LDHs at concentrations of 20 and 200 μg/mL, in contrast to other nanoparticles such as polystyrene and poly(ethylene glycol)-coated nanocapsules which induced moderate complement activation [33, 34]. Panas et al. reported that pre-coating of nanoparticles with serum or serum proteins prevented pro-inflammatory responses [35]. We

have previously reported that LDH can adsorb a large amount of albumin [36, 37], suggesting that LDH nanoparticles may attract more serum proteins than their neutrally charged counterparts (such as polystyrene). This protein coating on the LDH nanoparticle surface may limit their interactions with sensitive biomolecules such as complement proteins, and thus reduce subsequent complement activation.

4. Conclusions

This paper is the first to investigate the potential toxicity of LDH nanoparticles towards key components of the circulatory system, specifically vascular cells, RBCs and the complement system, based on *in vitro* and *ex vivo* screening tests. We conclude that MgAl-LDHs with a lateral diameter of *ca.* 100 nm have low toxicity, little effect on vascular cell growth, and negligible effect on the rupture of RBCs and complement activation. Thus MgAl-LDH nanomaterial has low cytotoxicity for vascular cells, high haemocompatiblity, and limited recognition by the innate immune system. Although future work (e.g. in *vivo* evaluation of biosafety) is needed to complete the biosafety profile of LDH nanoparticles, the present paper provides important insights into the biosafety of LDH nanoparticles, and expands the limited data available regarding LDH biosafety [38]. Importantly, we envisage that the *in vitro* and *ex vivo* assays described here could be used for the initial screening of nanomaterials for biosafety.

Acknowledgements

We would like to thank Mr. Al Dyne for assistance with the SMC isolation, Dr. Helga Manthey for helpful discussions regarding the complement activation assay, and Dr. Bing Zhang for performing an *ex vivo* complement assay trial. Part of this research used the facilities at the Electron Microscope Unit at UNSW. Financial support was provided by the National Health

and Medical Research Council (NHMRC) Early Career Fellowship (APP1073591) and the Australian Research Council (ARC) Future Fellowship (FT120100813).

References

[1] H.M. Chen, W.Z. Zhang, G.Z. Zhu, J. Xie, X.Y. Chen, Rethinking cancer nanotheranostics, Nat. Rev. Mater. 2 (2017) pp.18.
[2] P.S. Braterman, Z.P. Xu, F. Yarberry, Layered Double Hydroxides (LDHs), in: S.M. Auerbach, K.A. Carrado, P.K. Dutta (Eds.), Handbook of Layered Materials, Marcel Dekker, New York, 2004, pp. 373-474.
[3] Z.P. Xu, Q.H. Zeng, G.Q. Lu, A.B. Yu, Inorganic nanoparticles as carriers for efficient cellular delivery, Chem. Eng. Sci. 61 (2006) pp.1027-1040.
[4] Z.P. Xu, M. Niebert, K. Porazik, T.L. Walker, H.M. Cooper, A.P.J. Middelberg, P.P. Gray, P.F. Bartlett, G.Q. Lu, Subcellular compartment targeting of layered double hydroxide nanoparticles, J. Control. Release 130 (2008) pp.86-94.
[5] Z. Gu, B.E. Rolfe, A.C. Thomas, J.H. Campbell, G.Q. Lu, Z.P. Xu, Cellular trafficking of low molecular weight heparin incorporated in layered double hydroxide nanoparticles in rat vascular smooth muscle cells, Biomaterials 32 (2011) pp.7234-7240.
[6] Z. Gu, J.J. Atherton, Z.P. Xu, Hierarchical layered double hydroxide nanocomposites: structure, synthesis and applications, Chem. Commun. 51 (2015) pp.3024-3036.
[7] G. Choi, O.J. Kwon, Y. Oh, C.O. Yun, J.H. Choy, Inorganic nanovehicle targets tumor in an orthotopic breast cancer model, Sci. Rep. 4 (2014).
[8] Z. Gu, B.E. Rolfe, Z.P. Xu, A.C. Thomas, J.H. Campbell, G.Q.M. Lu, Enhanced effects of low molecular weight heparin intercalated with layered double hydroxide nanoparticles on rat vascular smooth muscle cells, Biomaterials 31 (2010) pp.5455-5462.
[9] Z. Gu, A.C. Thomas, Z.P. Xu, J.H. Campbell, G.Q. Lu, In vitro sustained release of LMWH from MgAl-layered double hydroxide nanohybrids, Chem. Mater. 20 (2008) pp.3715-3722.
[10] Z. Gu, A.H. Wu, L. Li, Z.P. Xu, Influence of hydrothermal treatment on physicochemical properties and drug release of anti-inflammatory drugs of intercalated layered double hydroxide nanoparticles, Pharmaceutics 6 (2014) pp.235-248.
[11] K. Ladewig, Z.P. Xu, G.Q. Lu, Layered double hydroxide nanoparticles in gene and drug delivery, Expert Opin. Drug Deliv. 6 (2009) pp.907-922.
[12] Y.Y. Wong, K. Markham, Z.P. Xu, M. Chen, G.Q. Lu, P.F. Bartlett, H.M. Cooper, Efficient delivery of siRNA to cortical neurons using layered double hydroxide nanoparticles, Biomaterials 31 (2010) pp.8770-8779.
[13] L. Li, W.Y. Gu, J. Liu, S.Y. Yan, Z.P. Xu, Amine-functionalized SiO2 nanodot-coated layered double hydroxide nanocomposites for enhanced gene delivery, Nano Res. 8 (2015) pp.682-694.
[14] W.Y. Chen, B. Zhang, T. Mahony, W.Y. Gu, B. Rolfe, Z.P. Xu, Efficient and Durable Vaccine against Intimin beta of Diarrheagenic E-Coli Induced by Clay Nanoparticles, Small 12 (2016) pp.1627-1639.
[15] H.L. Zuo, Z. Gu, H. Cooper, Z.P. Xu, Cross linking to enhance colloidal stability and redispersity of layered double hydroxide nanoparticles, J. Colloid Interface Sci. 459 (2015) pp.10-16.
[16] Z. Gu, B.E. Rolfe, Z.P. Xu, J.H. Campbell, G.Q. Lu, A.C. Thomas, Antibody-targeted drug delivery to injured arteries using layered double hydroxide nanoparticles, Adv. Healthc. Mater. 1 (2012) pp.669-673.

[17] B. Li, Z. Gu, N. Kurniawan, W.Y. Chen, Z.P. Xu, Manganese-Based layered double hydroxide nanoparticles as a T1-MRI contrast agent with ultrasensitive pH response and high relaxivity, Adv. Mater. 29 (2017).
[18] S.X. Shi, B.C. Fliss, Z. Gu, Y.A. Zhu, H. Hong, H.F. Valdovinos, R. Hernandez, S. Goel, H.M. Luo, F. Chen, T.E. Barnhart, R.J. Nickles, Z.P. Xu, W.B. Cai, Chelator-free labeling of layered double hydroxide nanoparticles for in vivo PET imaging, Sci. Rep. 5 (2015).
[19] D.E. Owens, N.A. Peppas, Opsonization, biodistribution, and pharmacokinetics of polymeric nanoparticles, Inter. J. Pharm. 307 (2006) pp.93-102.
[20] R.A. Majack, A.W. Clowes, Inhibition of vascular smooth muscle cell migration by heparin-like glycosminoclycans, J. Cell. Physiol. 118 (1984) pp.253-256.
[21] Y.S. Lin, C.L. Haynes, Impacts of mesoporous silica nanoparticle size, pore ordering, and pore integrity on hemolytic activity, J. Am. Chem. Soc. 132 (2010) pp.4834-4842.
[22] T. Yu, A. Malugin, H. Ghandehari, Impact of silica nanoparticle design on cellular toxicity and hemolytic activity, ACS Nano 5 (2011) pp.5717-5728.
[23] T.E. Mollnes, O.L. Brekke, M. Fung, H. Fure, D. Christiansen, G. Bergseth, V. Videm, K.T. Lappegard, J. Kohl, J.D. Lambris, Essential role of the C5a receptor in E-coli-induced oxidative burst and phagocytosis revealed by a novel lepirudin-based human whole blood model of inflammation, Blood 100 (2002) pp.1869-1877.
[24] D. Pavlovski, J. Thundyil, P.N. Monk, R.A. Wetsel, S.M. Taylor, T.M. Woodruff, Generation of complement component C5a by ischemic neurons promotes neuronal apoptosis, Faseb J. 26 (2012) pp.3680-3690.
[25] Z.P. Xu, N.D. Kurniawan, P.F. Bartlett, G.Q. Lu, Enhancement of relaxivity rates of Gd-DTPA complexes by intercalation into layered double hydroxide nanoparticles, Chem. Eur. J. 13 (2007) pp.2824-2830.
[26] M.A. Dobrovolskaia, S.E. McNeil, Immunological properties of engineered nanomaterials, Nat. Nanotech. 2 (2007) pp.469-478.
[27] J. Meng, M. Yang, F.M. Jia, Z. Xu, H. Kong, H.Y. Xu, Immune responses of BALB/c mice to subcutaneously injected multi-walled carbon nanotubes, Nanotoxicology 5 (2011) pp.583-591.
[28] D. Leu, B. Manthey, J. Kreuter, P. Speiser, P.P. DeLuca, Distribution and elimination of coated polymethyl [2-14C]methacrylate nanoparticles after intravenous injection in rats, J. Pharm. Sci. 73 (1984) pp.1433-1437.
[29] F. Zhao, Y. Zhao, Y. Liu, X. Chang, C. Chen, Cellular uptake, intracellular trafficking, and cytotoxicity of nanomaterials, Small 7 (2011) pp.1322-1337.
[30] S.M. Moghimi, A.J. Andersen, D. Ahmadvand, P.P. Wibroe, T.L. Andresen, A.C. Hunter, Material properties in complement activation, Adv. Drug Deliv. Rev. 63 (2011) pp.1000-1007.
[31] H.D. Manthey, T.M. Woodruff, S.M. Taylor, P.N. Monk, Complement component 5a (C5a), Int. J. Biochem. Cell Biol. 41 (2009) pp.2114-2117.
[32] A. Chanan-Khan, J. Szebeni, S. Savay, L. Liebes, N.M. Rafique, C.R. Alving, F.M. Muggia, Complement activation following first exposure to pegylated liposomal doxorubicin (Doxil): possible role in hypersensitivity reactions, Ann. Oncol. 14 (2003) pp.1430-1437.
[33] I. Hamad, O. Al-Hanbali, A.C. Hunter, K.J. Rutt, T.L. Andresen, S.M. Moghimi, Distinct polymer architecture mediates switching of complement activation pathways at the nanosphere-serum interface: implications for stealth nanoparticle engineering, ACS Nano 4 (2010) pp.6629-6638.
[34] N.M. Molino, K. Bilotkach, D.A. Fraser, D.M. Ren, S.W. Wang, Complement activation and cell uptake responses toward polymer-functionalized protein nanocapsules, Biomacromolecules 13 (2012) pp.974-981.
[35] A. Panas, C. Marquardt, O. Nalcaci, H. Bockhorn, W. Baumann, H.R. Paur, S. Mulhopt, S. Diabate, C. Weiss, Screening of different metal oxide nanoparticles reveals selective toxicity

and inflammatory potential of silica nanoparticles in lung epithelial cells and macrophages, Nanotoxicology 7 (2013) pp.259-273.
[36] Z. Gu, H.L. Zuo, A.H. Wu, Z.P. Xu, Stabilization of layered double hydroxide nanoparticles by bovine serum albumin pre-coating for drug/gene delivery, J. Control. Release 213 (2015) pp.E150-E151.
[37] Z. Gu, H.L. Zuo, L. Li, A.H. Wu, Z.P. Xu, Pre-coating layered double hydroxide nanoparticles with albumin to improve colloidal stability and cellular uptake, J. Mat. Chem. B 3 (2015) pp.3331-3339.
[38] S.J. Choi, J.M. Oh, J.H. Choy, Safety aspect of inorganic layered nanoparticles: Size-dependency in vitro and in vivo, J. Nanosci. Nanotechnol. 8 (2008) pp. 5297-5301.

Figure Captions

Fig. 1 (A) TEM image of the LDH nanoparticles with the insert STEM image; (B-E) the elemental mapping of (B) Mg, (C) Al and (D) O of LDHs (E: overlays of Mg, Al and O maps); (F) hydrodynamic size distribution and (G) powder X-ray diffraction pattern of LDH nanoparticles.

Fig. 2 Cell proliferation (A, B) and cell viability (C, D) of SMC or HUVEC treated with LDH at concentrations from 10 to 500 μg/mL. The dashed line indicates the percentage of cells at the start of treatment. (** $p \leq 0.01$, *** $p \leq 0.001$)

Fig. 3 SMC migration following LDH treatment. Fluorescence images (A) show SMC migration after 4-day treatment with culture medium containing PBS or LDH. Cytoplasm was visualized with CellTracker Green (green), and nuclei with Hoechst 33342 (blue); the interrupted lines show the original scratch line. Phase contrast images show SMC monolayers immediately after scratch wounding (D0). Scale bar = 100 μm. Bar graphs (B) show the proportion of migrating cells in each treatment (PBS/control or LDH).

Fig. 4 Photograph (A) and percent haemolysis (B) of RBCs incubated with LDH nanoparticles (25-400 μg/mL) for 3 hours at 37 ^{o}C. (+) and (-) in (A) indicate positive and negative control respectively, and 100% in (B) represents the percent haemolysis of positive control.

Fig. 5 *Ex vivo* complement activation assay. C5a levels in lepirudin-treated mouse plasma following incubation with LDH nanoparticles (20 or 200 μg/mL).

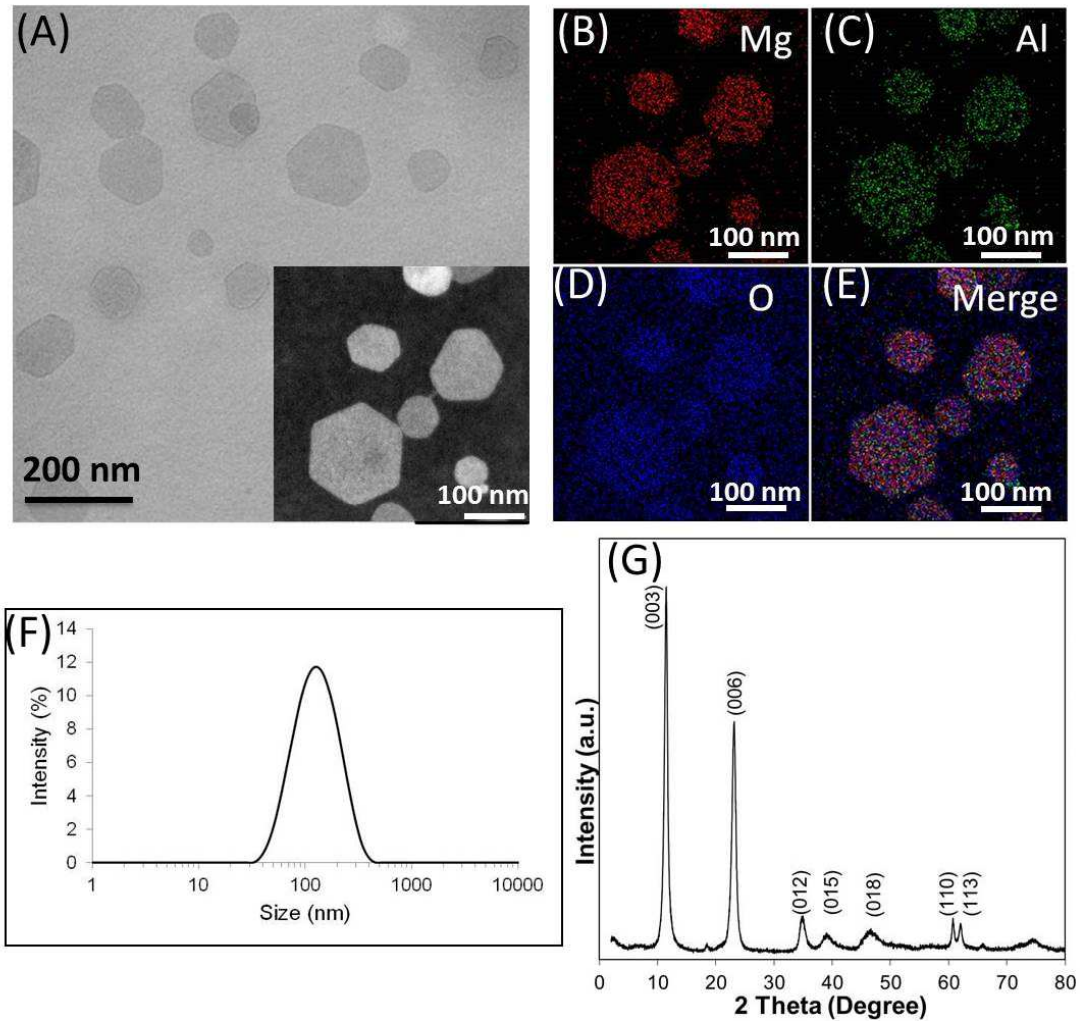
(A)
200 nm
100 nm
(B)
Mg
100 nm
(C)
Al
100 nm
(D)
O
100 nm
(E)
Merge
100 nm
(F)
Intensity (%)
Size (nm)
(G)
Intensity (a.u.)
(003)
(006)
(012)
(015)
(018)
(110)
(113)
2 Theta (Degree)

Fig. 1

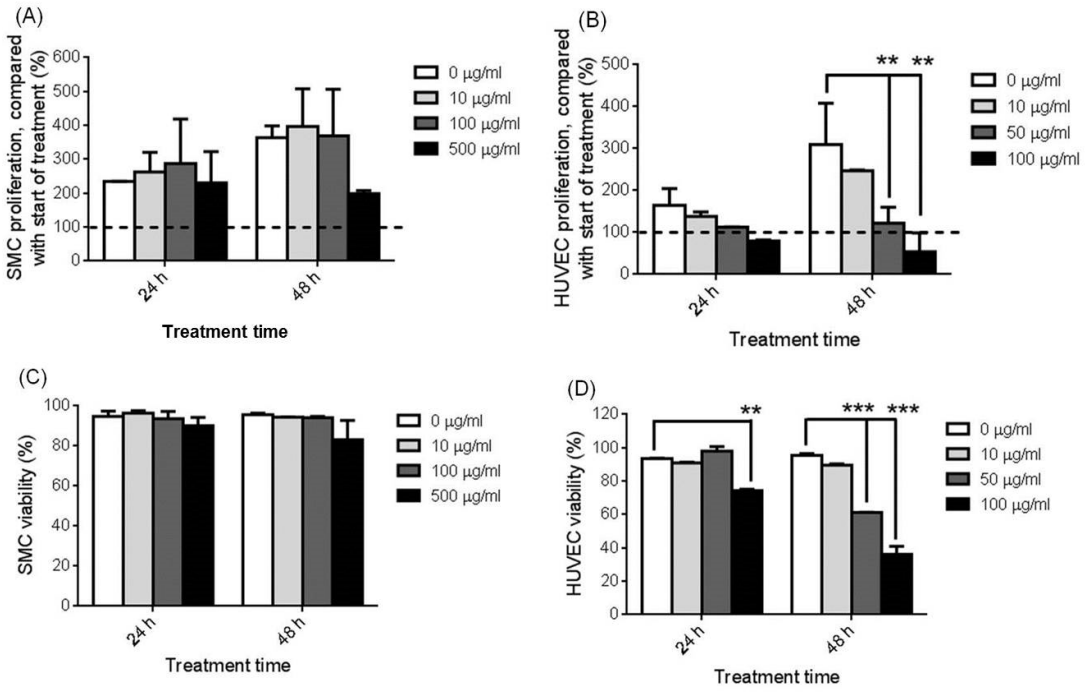
(A)
SMC proliferation, compared with start of treatment (%)
600
500
400
300
200
100
0
24 h
48 h
Treatment time
0 µg/ml
10 µg/ml
100 µg/ml
500 µg/ml
(B)
HUVEC proliferation, compared with start of treatment (%)
500
400
300
200
100
0
** **
24 h
48 h
Treatment time
0 µg/ml
10 µg/ml
50 µg/ml
100 µg/ml
(C)
SMC viability (%)
100
80
60
40
20
0
24 h
48 h
Treatment time
0 µg/ml
10 µg/ml
100 µg/ml
500 µg/ml
(D)
HUVEC viability (%)
120
100
80
60
40
20
0
**
*** ***
24 h
48 h
Treatment time
0 µg/ml
10 µg/ml
50 µg/ml
100 µg/ml

Fig. 2

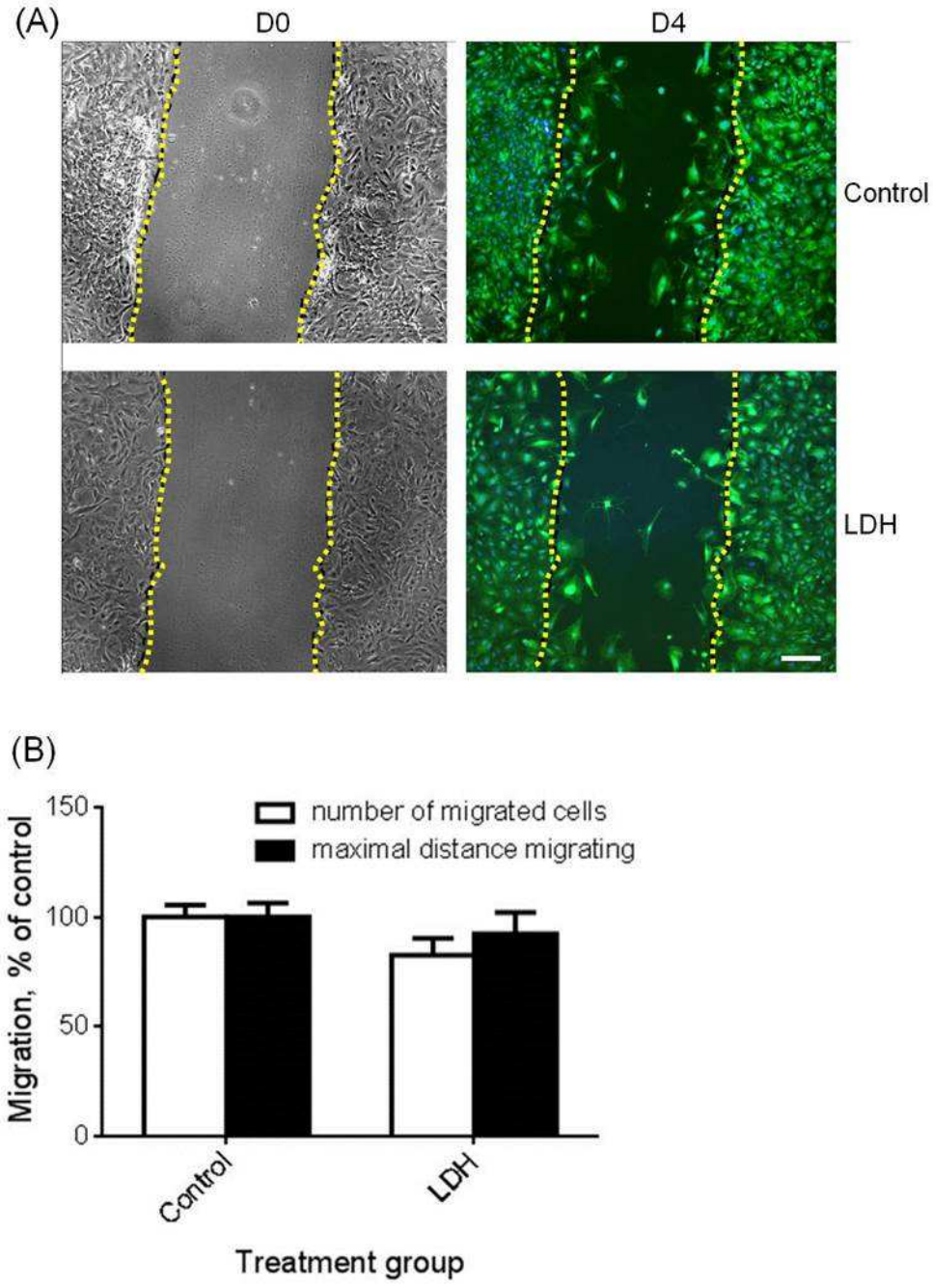
(A)
D0
D4
Control
LDH
(B)
number of migrated cells
maximal distance migrating
Migration, % of control
150
100
50
0
Control
LDH
Treatment group

Fig. 3

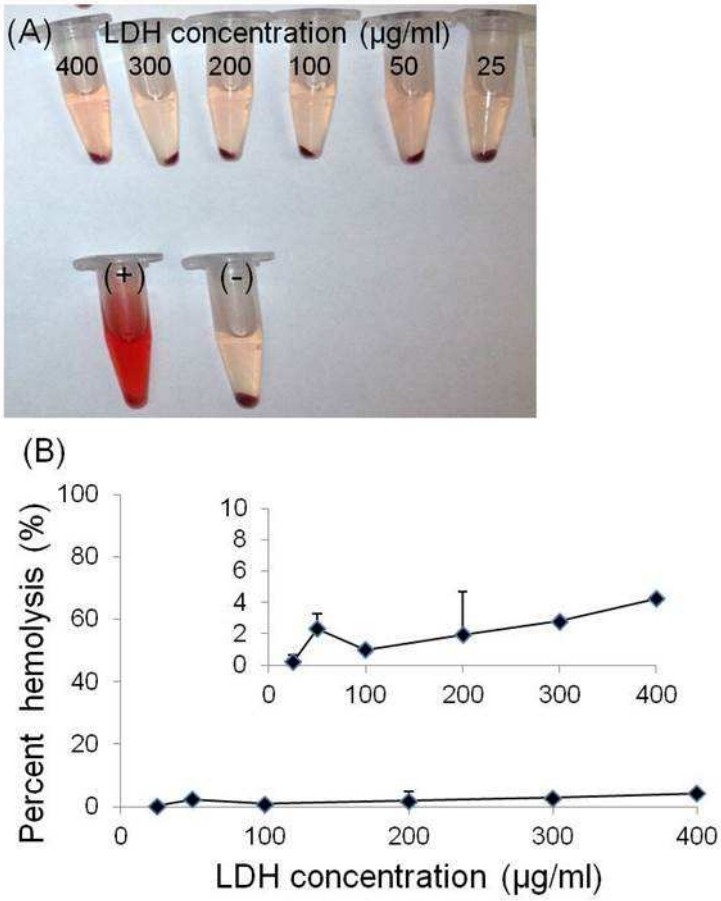
(A)
LDH concentration (μg/ml)
400
300
200
100
50
25
(+)
(-)
(B)
Percent hemolysis (%)
100
80
60
40
20
0
0
100
200
300
400
10
8
6
4
2
0
0
100
200
300
400
LDH concentration (μg/ml)

Fig. 4

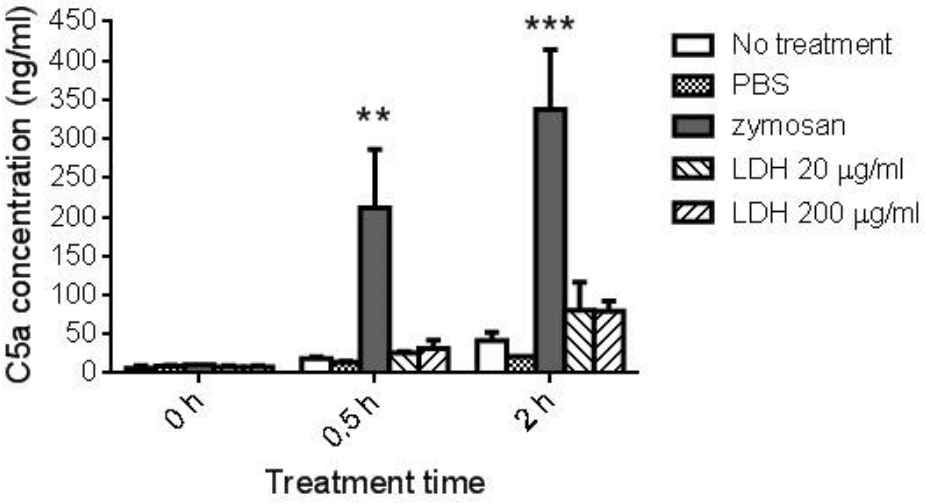
C5a concentration (ng/ml)
450
400
350
300
250
200
150
100
50
0
**
***
0 h
0.5 h
2 h
Treatment time
No treatment
PBS
zymosan
LDH 20 µg/ml
LDH 200 µg/ml

Fig. 5